https://doi.org/10.3311/PPee.38223

Periodica Polytechnica Electrical Engineering and Computer Science, 69(2), pp. 159–166, 2025

Numerical Study of the Optimal Position of Corona Wires in Two Types of ESP

Moath Bani Fayyad[1*], Tamás Iváncsy[1]

[1] Department of Electric Power Engineering, Faculty of Electrical Engineering and Informatics, Budapest University of Technology and Economics, Műegyetem rkp. 3., H-1111 Budapest, Hungary
[*] Corresponding author, e-mail: mbanifayyad@edu.bme.hu

Received: 29 August 2024, Accepted: 11 February 2025, Published online: 21 February 2025

Abstract
In recent years, particulate emissions have advanced to the top of the global priority list. Numerous research, both numerical and experimental, have been conducted to explore different corona wires and collecting plate configurations. This study aims to investigate the best location of corona wires arrangements using 3 types of collecting plates; wavy plates (wavyPs), and inverted wavy plates (InvwavyPs), flat plates (FPs) as a reference case. Where, three positions of corona arrangements were modelled with three types of collecting plates *via* Finite Element Method (FEM).

Keywords
corona wires, COMSOL multiphysics, electrostatic precipitator (ESP), Finite Element Method (FEM)

1 Introduction

Particulate emissions are one of the most significant problems with air pollution, and they have become a major concern for everyone. Electrostatic precipitators (ESPs) are often used to filter out airborne pollutants in various industrial applications. ESPs are often used in several industrial applications to capture particles that should not be discharged into the atmosphere. Although the particle removal efficiency for tiny particles (about 0.2 μm) has been very low, ESPs may attain over 99% efficiency and need relatively little energy to operate [1–6].

ESPs are often classified into two categories based on the number of stages and the geometric configuration of their collecting plates. ESPs can be categorized as either single-stage or two-stage, depending on the number of steps in the charging and collecting sections. ESPs can be categorized as plate-type, tubular, and wire-type, depending on the physical arrangement of their collection plates. Plate-type ESPs utilize flat or corrugated plates to collect particles, whereas tubular ESPs use cylindrical tubes, and wire-type ESPs use wires to generate an ionizing corona that charges the particles [7].

Numerous research, both numerical and experimental, have been conducted to explore different ESP collecting plate configurations; for instance, flat plates (FPs) and related arrangements are investigated [5, 8–13]. Different shapes of collecting plates were numerically studied such as C-type, wavy, triangular, and W-type, and crenelated plates [1–6, 14–17]. Electric field parameters, airflow distribution uniformity, and collection efficiency were examined for seven dust-collecting plates [18].

The aim of this study is investigating the effect of the corona wire position on the performance of the single-stage ESP based on this study [4], where they discussed the wavy configurations of collecting electrodes in a single-stage ESP. According to the research conducted by Choi et al. [16], it was found that there is a positive correlation between the increase in applied voltage and the improvement in collection efficiency. Nevertheless, the augmentation of the volumetric volume has a detrimental impact on the collecting efficiency [16]. The utilization of wavy plates in particle charging and transport is enhanced by directing attention to the wavy design. The study identified the wavy-E case design as having the performance most close to optimal, with a value of (λ/the ratio of the wavelength / the distance between two corona wires (Lww)) equal to 1 and (A/the ratio of the Amplitude / the distance between the corona wire and the collecting plate (Lwp)) equal to 0.3 [16]. In addition,

Cite this article as: Bani Fayyad, M., Iváncsy, T. "Numerical Study of the Optimal Position of Corona Wires in Two Types of ESP", Periodica Polytechnica Electrical Engineering and Computer Science, 69(2), pp. 159–166, 2025. https://doi.org/10.3311/PPee.38223

Gao et al. [19] investigated the phenomenon of particle migration by employing various electrode configurations [19]. Their findings indicate that modifying the forms of the corona electrodes and collecting plates substantially impacts the electrical properties related to this process [19].

2 Physical model

ESPs employ electric fields to eliminate dust and particles from the air. The technique involves ionizing molecules, which results in the charge of dust particles in the air and their subsequent attraction towards collection plates. The system integrates gas flow, electric fields, dust particle charge, movement, and collection [2].

2.1 Gas flow

The performance of particle collection is determined by the kind of gas flow, with laminar flow following an algebraic rule and turbulent flow following a probability exponential law [20]. In this work, the proposed model was implemented as a laminar flow. The laminar flow is considered to be an ideal flow, which is governed by frictional or viscous forces. The flow as a laminar flow depends on the Reynolds number (Re), where the laminar flow is determined to be less than 2000. The Re is calculated using the formula:

$$\mathrm{Re} = \frac{\rho u_f L}{\mu_f}, \tag{1}$$

where Re is the Reynolds number, ρ is the density of the fluid, u_f is the velocity of the fluid relative to the object, L is a characteristic length (e.g., the diameter of a pipe or length of an object), and μ_f is the dynamic viscosity of the fluid.

This flow type is determined by the Navier-Stokes equations, which are used to conserve momentum and mass. This research is confined to an incompressible flow, which is described by the equation $\rho \nabla \boldsymbol{u} = 0$, representing the motion continuity. The momentum equation for laminar flow is determined by the fluid's velocity and pressure [1–6]:

$$\begin{aligned} &\rho \frac{\partial \boldsymbol{u}}{\partial t} + \rho\left(\boldsymbol{u} \times \nabla\right)\boldsymbol{u} \\ &= \nabla \times \left[-pI + \mu\left(\nabla \boldsymbol{u} + \left(\nabla \boldsymbol{u}\right)^T\right)\right] + \boldsymbol{F_{EHD}}, \end{aligned} \tag{2}$$

where ρ (kg/m^3) is the fluid density, p (Pa) is the pressure, μ (kg/(m s)) is the dynamic viscosity, and $\boldsymbol{F_{EHD}}$ is the electrohydrodynamic force vector [1–6].

2.2 Electrostatic field

The electrostatic model for the ESP is characterized by charge conservation and poisson equations:

$$\frac{\partial \rho_q}{\partial t} + \nabla \times \boldsymbol{J} = 0, \tag{3}$$

$$\boldsymbol{J} = z_q \mu \rho_q \boldsymbol{E} + \rho \boldsymbol{u}, \tag{4}$$

$$\varepsilon_0 \nabla^2 V = -\rho_q, \tag{5}$$

$$\boldsymbol{E} = -\nabla V, \tag{6}$$

where ρ_q (C m^{-3}) is the space charge number density, $\boldsymbol{J}$ (A m^{-2}) is the current density vector, z_q is the charge number, μ (m^2 V^{-1} s^{-1}) is the ion mobility, $\boldsymbol{E}$ (V m^{-1}) is the electric field intensity vector, $\boldsymbol{u}$ (m s^{-1}) is the fluid velocity vector, ε_0 (F m^{-1}) is the free-space permittivity, and V (V) is the electric potential [21].

2.3 Particle charging and particle and kinetics

The charging of particles in ESPs is a multifaceted phenomenon that takes place at the interface of the negative electrode surface and the active plasma region [22]. This phenomenon is regulated by two fundamental charging mechanisms, namely diffusion charging and field charging [21]. Diffusion charging is based on Brownian motion [23]. Diffusion charging is predominant for particles smaller than 0.5 µm, while field charging is predominant for particles larger than 1 µm [20, 24].

2.4 Particle collection

Particle collection consists of the charged particles propelled towards the plates by the electric field. The trajectory of larger particles in the direction of the plate can be detected using the average gas velocity and average particle velocity. The efficiency of the ESP can be assessed by evaluating parameters such as current-voltage characteristics (I–V), corona power ratio [25], optimization of geometrical characteristics (electrode geometry, wire radius, wire-wire distance, collecting electrode geometry, shape, and distance [26]. Other factors to consider are pre-charge length to collecting stage length ratio, EHD flow, airflow velocity, power consumption, and number of corona wires [26].

The majority of empirical relationships have been implemented in the development of industrial-scale ESPs capable of effectively achieving superior performance in particle collection. Deutsch described the equation of the particle collection efficiency for the single-stage duct type based on the probability theory as Eq. (7); where $\boldsymbol{v}$ (m/s) is the particle velocity vector. Equation (7) is used to calculate the particle collection efficiency with ideal conditions and several assumptions [22].

$$\eta = 1 - \exp\left(-\frac{L \times |\boldsymbol{v}|}{s \times |\boldsymbol{u}|}\right) \tag{7}$$

2.5 The proposed design

In this study, three models of wavy plates, inverted wavy plates (InvwavyPs) and FPs, as a reference model based on the wavy-E case, were investigated with three positions of corona wires which have the same Lww [4], which provided better performance. The inverted wavy shape is used to check what happens when the wavy shape is reversed. The work's findings demonstrate how the electric potential, electric field strength, current density, space charge density distribution, and particle collection efficiency are affected by varying the corona position when wavy and inverted wavy collecting electrodes are utilized. Based on the results (Fig. 1), it has been demonstrated that the wavy plates (wavyPs) exhibit superior overall performance in the specific range of particles (0.01−5 μm), higher than both the InvwavyPs and FPs in position 1 (P1). Meanwhile, the higher particle collection efficiency in position 3 (P3) is InvWavyPs, which provided an additional possibility of applied voltage above 20 kV. In position 2 (P2), the particle collection efficiency of wavyPs is higher than that of InvwavyPs.

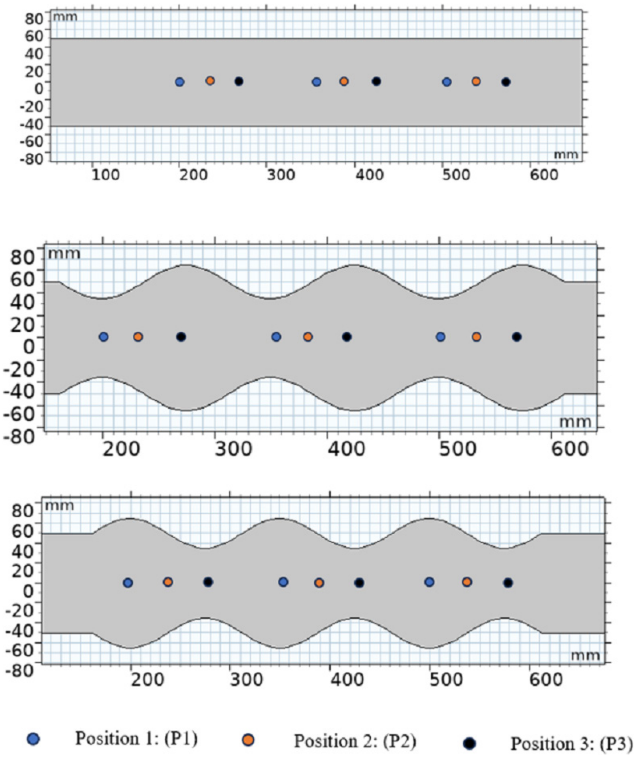

Fig. 1 Geometrical arrangements with 3 positions of corona wires using FP, wavyP, and InvWavyP

3 Results and discussion

3.1 The electrical potential and electrical field

The simulation supplies the corona electrodes with an electric potential of 20 kV as specified in the Table 1. In contrast, the collecting electrodes are provided with a potential of 0 V. To understand the behavior of the electrical potential distribution in FPs, wavyPs, and InvwavyPs, Fig. 2 shows the electrical potential distributions for three types of ESP. Several observations can be made, such as the electric potential levels near corona wires exhibiting a different pattern when observed in the wavy plates as opposed to flat plates. The circular shape of the potential distribution in the adjacent corona electrodes is greater when employing flat plates compared to wavy plates. In this design, the high electric potential values in the direction of the collecting plates are reduced. While in the InvwavyPs, the potential distribution of the corona wires exhibits a reduced magnitude and a more circular shape in comparison to flat plates potential values are observed to be nearly symmetrical and located near the center of the corona wires.

In this investigation, three different positions of corona wires with the same Lww were selected; P1, P2, and P3. The study aims to comprehend the impact of changing the position on the distributions of electric potential and other electrical properties. Cut lines were created at $x = 350$ mm for P1, $x = 387.5$ mm for P2, and $x = 425$ mm for P3 to see

Table 1 ESP's parameters for 3 types of collecting plates

Description	Value
Width (mm)	700
Distance between the collecting plates (mm)	100
Distance between two corona wires (mm)	150
Number of corona electrodes	3
Corona electrode radius (mm)	0.5
Applied voltage (kV)	20
Air laminar fluid flow, avg velocity (m/s)	1
Temperature (K)	293.15
Gas density (kg m^{-3})	1.2
Gas viscosity (Pa s)	2.57×10^{-7}
Pressure (atm)	1
Particle radii (μm)	0.01−5
Particle density (kg m^{-3})	2200
Particle relative permittivity	5

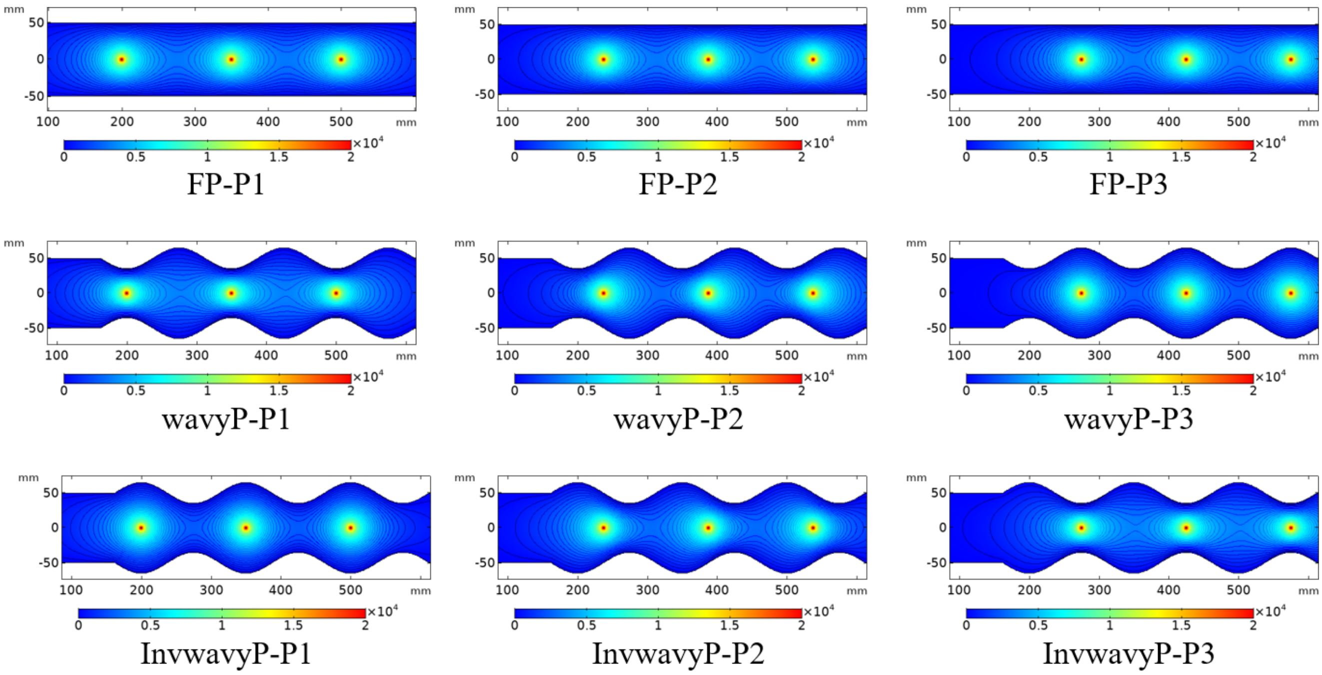

Fig. 2 Electric potential using different collecting plates with three positions

how the electric potential distribution behaves in the vertical direction.

Given that each design employs a unique shape, the distributions of electrical potential according to the vertical cutlines are shown in Fig. 3. As a result, the distance between a collecting plate and the corona wire is higher with InvwavyPs and shortest with wavyPs due to geometric arrangements for position P1. A more linear electric potential distribution is observed with FP with three positions of corona wires.

On the other hand, we can see the distributions of the electrical field with respect to the horizontal cutline at $y = 30$ mm as shown in Fig. 4. Using the inverse proportionality concept between the electrical field and the distance, more significant magnitudes of the electric field will be present in the case of wavyPs and lower magnitudes in the case of InvwavyPs for P1. A horizontal cut is defined at $y = 30$ mm due to the physical shape of the collecting plates; in Fig. 4, this magnitude distribution is observed for FPs, wavyPs, and InvwavyPs using three corona wires positions. The electric field distributions in FPs are symmetrical for P1, P2, and P3 due to the even shape of the collecting plates. However, for the wavyPs, the highest electric field distribution value is P1, then P2, and the smallest is P3. On the other hand, for InvwavyPs, P3 is the largest value of electrical field distribution.

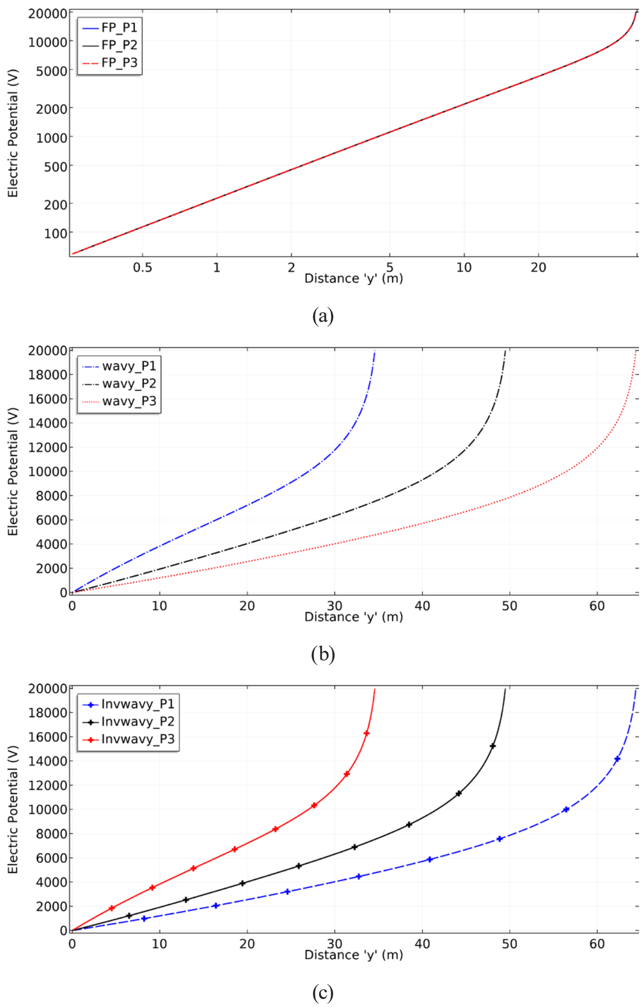

Fig. 3 Electric potential curves according to vertical cutline for (a) FPs, (b) wavyPs, and (c) InvwavyPs using three positions of corona wires

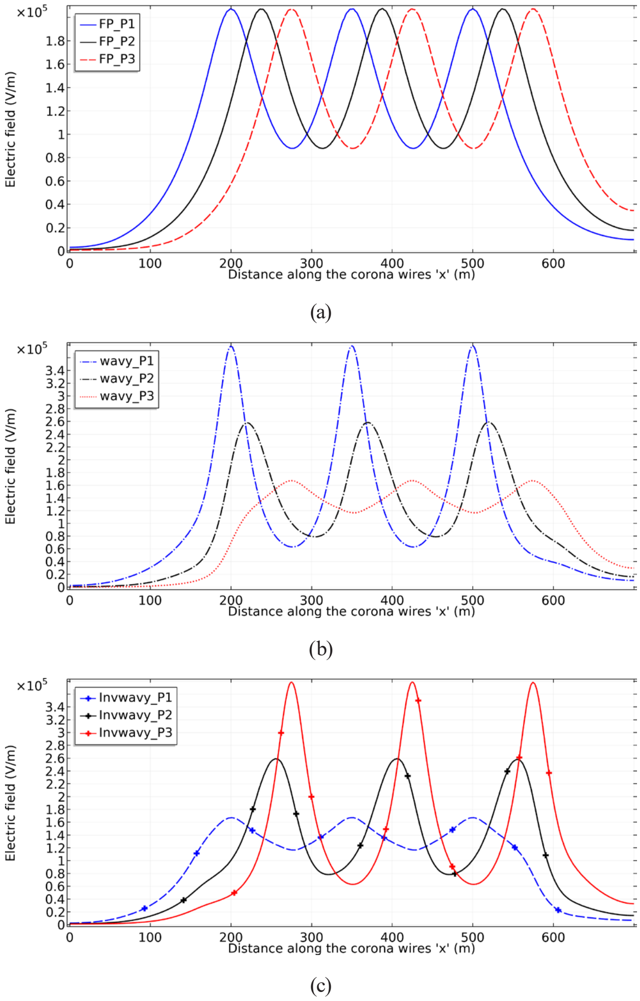

Fig. 4 Electric field curves according to horizontal cutline for (a) FPs, (b) wavyPs, and (c) InvwavyPs using three positions of corona wires

3.2 The space charge density and current density

The one of the primary objectives of this research considers comprehending the spatial arrangement of space charge density (ρ), which represents the quantity of charge contained inside a specified region. The visual representation of the ESP is depicted in Fig. 5. When looking at this electric property, it's clear that the highest levels of space charge density are grouped together in a small circle near the corona wires on all three types of collecting plates, with different distributions for all positions of the corona wires. It is important to remember that the corona discharge happens in a small area around the corona wires based on Peek's law.

Fig. 6 displays the space charge density according to the length of ESP. The data was gathered using a cutline of $y = 30$ mm, and the distribution form is the same for all three types of collecting plates. The highest levels of space charge density are found on wavyPs at P1 and InvwavyPs at P3. Regarding the ρ values at P2, both wavyPs and InvwavyPs designs have approximately the same values. Fig. 7 shows the distribution of current density using three types at $y = 30$ mm.

3.3 The particle collection efficiency

The principal objective of our study was to investigate the impact of modifications in geometric configurations of collecting plates and corona wires on particle collection efficiency. Three types of collecting plates were used with three positions (P1, P2, and P3). The evaluation of wavy collecting plates showed a superior capability for particle collection at P1, whereas InvwavyPs demonstrated a reduction in their ability to collect particles at P1. On the other hand, the best performance of particle collection efficiency at P3 is when using InvwavyPs. Regarding position P2, all the types have approximately the same performance. These results can be illustrated as the particle collection efficiency for three positions of corona wires within the range of particle radii 0.01–5 µm in Fig. 8.

Upon further examination of the results, the size of the corona wire also plays a significant role in the ESP performance. After investigating the position of corona wires in wavyPs, the influence of changing the corona wire radii in the wavyPs and InvwavyPs was investigated in [4, 5]. Using the position P1, three types of collecting plates (FP, wavyP, and InvwavyP) were compared to understand the relationship between the corona radius and the ESP particle collection efficiency. The relationship between the corona wires' radius and the electric field's distribution is inversely proportional. The findings of this study indicate that the most significant electric field magnitudes are produced by the corona electrodes with the smallest radii [4, 5].

4 Conclusion

This study examined three models of wavy plates, InvwavyPs, and FPs as a reference model based on the wavy-E case with three positions of corona wires with the same Lww, which performed superior. With the inverted wavy form, you can observe what occurs when you reverse it. The results of the study illustrate the impact of variation in the corona position on the electric potential, electric field strength, current density, space charge density distribution, and particle collection efficiency when wavy and inverted wavy collecting electrodes are employed. The results show that the wavyPs outperform the InvwavyPs and FPs in position 1 (P1) in terms of overall performance within the specified range of particles (0.01–5 µm). InvWavyPs has a greater particle collecting efficiency in position 3 (P3), allowing applied voltage exceeding 20 kV. In position 2 (P2), wavyPs capture particles better than InvwavyPs.

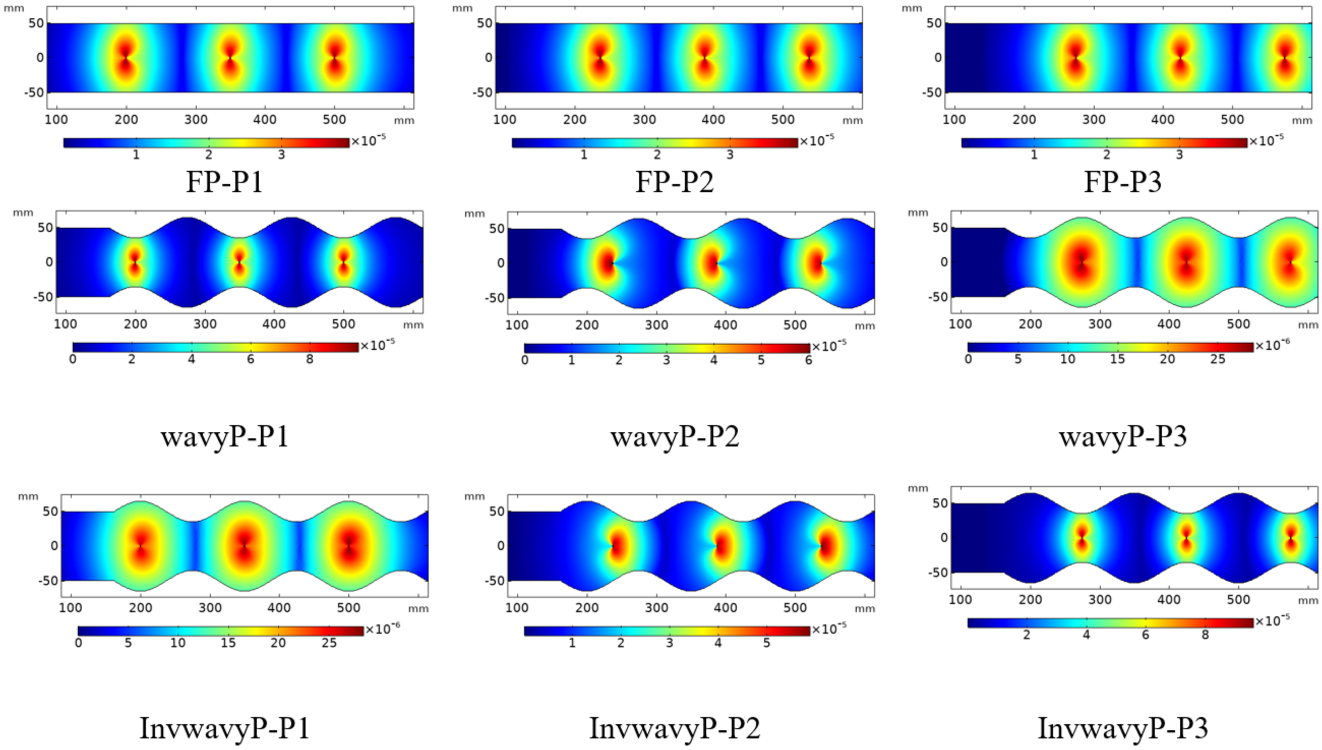

Fig. 5 Space charge density in FPs, wavyPs, and InvwavyPs

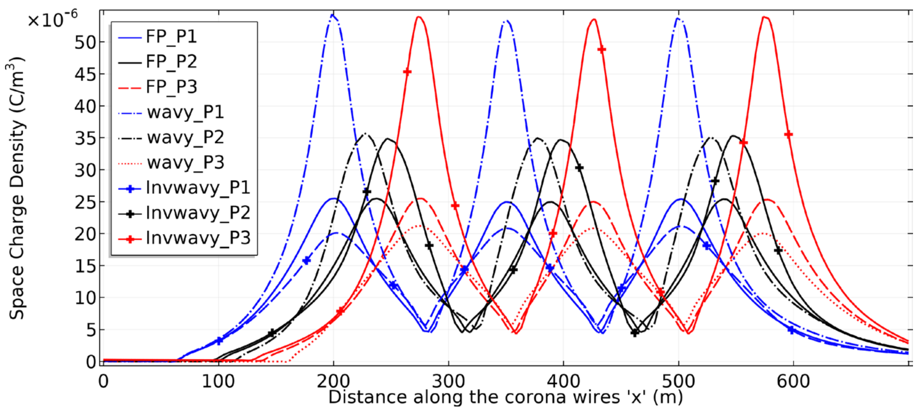

Fig. 6 Space charge density in FPs, wavyPs, and InvwavyPs

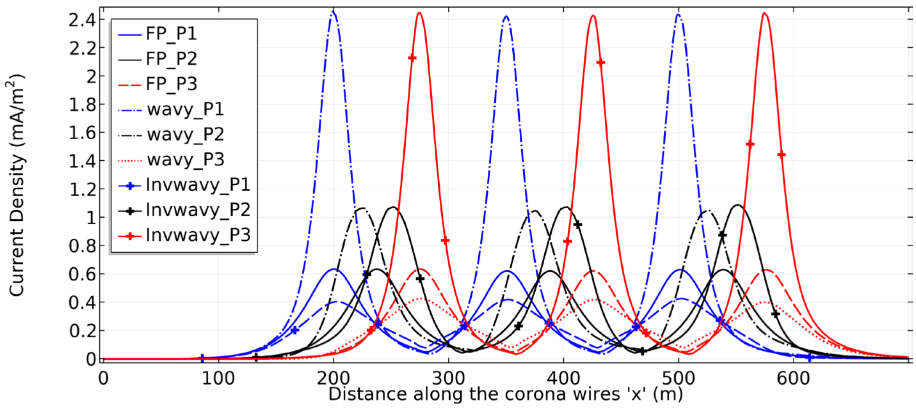

Fig. 7 Current charge density in FPs, wavyPs, and InvwavyPs

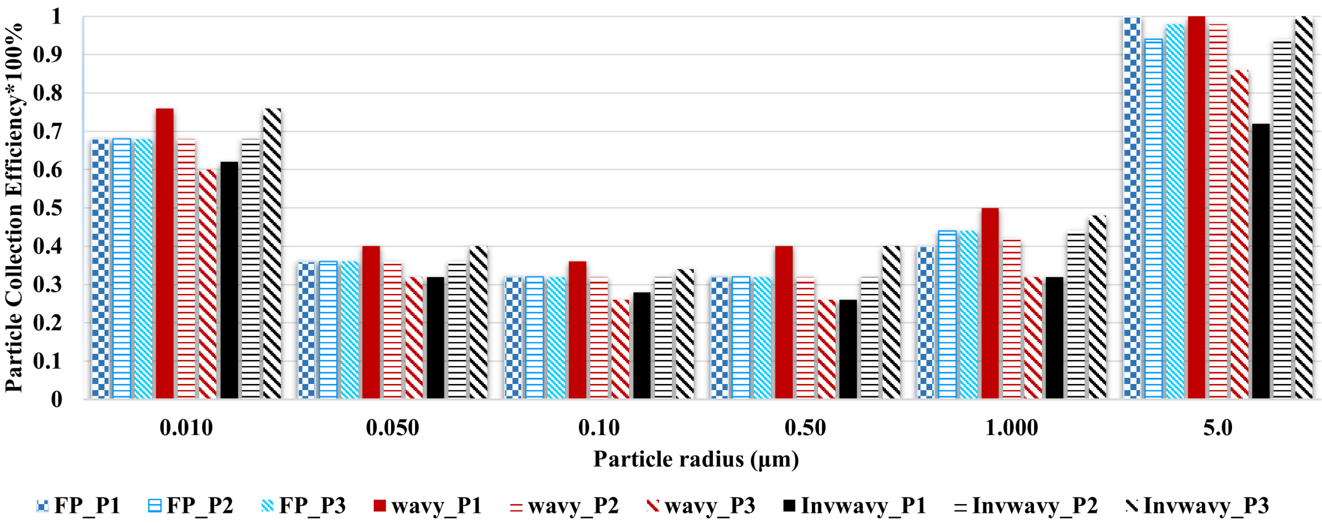

Fig. 8 Particle collection efficiency results using flat, wavy, and inverted wavy collecting plates for three positions

However, this study will lead to explore additional research of different types, to obtain the optimal design of ESP collecting electrodes and corona wires.

Acknowledgement

The project presented in this article is supported by Stipendium Hungaricum.

References

[1] Bani Fayyad, M. M., Asipuela González, A. G., Iváncsy, T. "Numerical study of wavy collecting electrodes with different shapes of corona electrodes", In: 2022 IEEE 5th International Conference and Workshop Óbuda on Electrical and Power Engineering (CANDO-EPE), Budapest, Hungary, 2022, pp. 000037–000042. ISBN 979-8-3503-4620-6
https://doi.org/10.1109/CANDO-EPE57516.2022.10046364

[2] Fayyad, M. B., González, A. A., Iváncsy, T. "The effects of the corona wire distribution with triangular collecting plates on the characteristics of electrostatic precipitators", In: 2022 International Conference on Diagnostics in Electrical Engineering (Diagnostika), Pilsen, Czech Republic, 2022, pp. 1–7. ISBN 978-1-6654-8083-3
https://doi.org/10.1109/Diagnostika55131.2022.9905103

[3] Fayyad, M. B., González, A. A., Iváncsy, T. "Numerical study of a duct-type ESP with W-type collecting electrodes and different circular corona electrodes radius", In: 2022 8th International Youth Conference on Energy (IYCE), Eger, Hungary, 2022, pp. 1–5. ISBN 978-1-6654-8722-1
https://doi.org/10.1109/IYCE54153.2022.9857530

[4] Asipuela González, A. G., Bani Fayyad, M., Iváncsy, T. "The Effect of Corona Wire Position and Radius in a Duct-Type ESP with Wavy Collecting Plates", International Journal of Electrical and Electronic Engineering & Telecommunications, 11(4), pp. 262–268, 2022.
https://doi.org/10.18178/ijeetc.11.4.262-268

[5] Asipuela, A., Fayyad, M. B., Iváncsy, T. "Study and Numerical Simulation of a Duct-type ESP with Wavy Collecting Electrodes and Different Circular Corona Electrodes Radius", In: 2022 IEEE 4th International Conference on Dielectrics (ICD), Palermo, Italy, 2022, pp. 234–238. ISBN 978-1-6654-1834-8
https://doi.org/10.1109/ICD53806.2022.9863610

[6] Fayyad, M. B., González, A. A., Iváncsy, T. "Numerical study of the influence of using crenelated collecting plates on the electrostatic precipitators", Journal of Electrostatics, 123, 103811, 2023.
https://doi.org/10.1016/j.elstat.2023.103811

[7] Bani Fayyad, M., Iváncsy, T. "Numerical Study of the Influence of Using Semicircular Corrugated Collecting Plate and Inverted Semicircular Corrugated on the Electrostatic Precipitator", Periodica Polytechnica Electrical Engineering and Computer Science, 68(2), pp. 124–134, 2024.
https://doi.org/10.3311/PPee.22592

[8] Fujishima, H., Ueda, Y., Tomimatsu, K., Yamamoto, T. "Electrohydrodynamics of spiked electrode electrostatic precipitators", Journal of Electrostatics, 62(4), pp. 291–308, 2004.
https://doi.org/10.1016/j.elstat.2004.05.006

[9] Wang, J., Cai, Y., Li, X., Shi, Y., Bao, Y. "Electrically-induced ionic wind flow distribution and its application for LED cooling", Applied Thermal Engineering, 138, pp. 346–353, 2018.
https://doi.org/10.1016/j.applthermaleng.2018.04.091

[10] Lami, E., Mattachini, F., Gallimberti, I., Turrib, R., Tromboni, U. "A numerical procedure for computing the voltage-current characteristics in electrostatic precipitator configurations", Journal of Electrostatics, 34(4), pp. 385–399, 1995.
https://doi.org/10.1016/0304-3886(94)00030-Z

[11] Parker, K. "Electrical Operation of Electrostatic Precipitators", The Institution of Engineering and Technology (IET), 2003. ISBN 978-0-85296-137-7
https://doi.org/10.1049/PBPO041E

[12] Wen, T.-Y., Krichtafovitch, I., Mamishev, A. V. "Numerical study of electrostatic precipitators with novel particle-trapping mechanism", Journal of Aerosol Science, 95, pp. 95–103, 2016. https://doi.org/10.1016/j.jaerosci.2016.02.001

[13] Zhu, Y., Gao, M., Chen, M., Shi, J., Shangguan, W. "Numerical simulation of capture process of fine particles in electrostatic precipitators under consideration of electrohydrodynamics flow", Powder Technology, 354, pp. 653–675, 2019. https://doi.org/10.1016/j.powtec.2019.06.038

[14] Lami, E., Mattachini, F., Sala, R., Vigl, H. "A mathematical model of electrostatic field in wires-plate electrostatic precipitators", Journal of Electrostatics, 39(1), pp. 1–21, 1997. https://doi.org/10.1016/S0304-3886(96)00044-7

[15] Fayyad, M. B., Asipuela, A., Iváncsy, T. "The effect of the corona wire distribution with W-type of collecting plates on the characteristics of electrostatic precipitators", Journal of Electrostatics, 125, 103841, 2023. https://doi.org/10.1016/j.elstat.2023.103841

[16] Choi, H. Y., Park, Y. G., Ha, M. Y. "Numerical simulation of the wavy collecting plate effects on the performance of an electrostatic precipitator", Powder Technology, 382, pp. 232–243, 2021. https://doi.org/10.1016/j.powtec.2020.12.070

[17] Zhou, W., Jiang, R., Sun, Y., Chen, B., Liu, B. "Study on multi-physical field characteristics of electrostatic precipitator with different collecting electrodes", Powder Technology, 381, pp. 412–420, 2021. https://doi.org/10.1016/j.powtec.2020.12.028

[18] Chen, B., Guo, Y., Li, H., Liu, B., He, Y., Zhao, H. "Insights into the effect of the shape of collecting plates on particle precipitation processes in an electrostatic precipitator", Journal of the Air & Waste Management Association, 70(9), pp. 892–903, 2020. https://doi.org/10.1080/10962247.2020.1768965

[19] Gao, W., Wang, Y., Zhang, H., Guo, B., Zheng, C., Guo, J., Gao, X., Yu, A. "Numerical simulation of particle migration in electrostatic precipitator with different electrode configurations", Powder Technology, 361, pp. 238–247, 2020. https://doi.org/10.1016/j.powtec.2019.08.046

[20] White, H. J. "Industrial Electrostatic Precipitation", Addison-Wesley Publishing Company, Reading, MA, USA, 1963.

[21] COMSOL "Electrostatic Precipitator", [online]. Available at: https://www.comsol.com/model/electrostatic-precipitator-71361 [Accessed: 31 December 2020]

[22] Fuliful, F. K., Hamood, A. A. "Collection Efficiency of Wire-Duct Electrostatic Precipitator", LAP LAMBERT Academic Publishing, 2017. ISBN 978-3659936432

[23] Richards, J. "Apti Course 413: Control of Particulate Emissions: Student Manual", North Carolina State University, 1995. ISBN 9781560490241

[24] Asipuela González, A., Fayyad, M. B., Iváncsy, T. "The effect of combining wavy and W-type collecting electrodes on the properties of electrostatic precipitators", Journal of Electrostatics, 123, 103818, 2023. https://doi.org/10.1016/j.elstat.2023.103818

[25] Ning, Z., Podlinski, J., Shen, X., Li, S., Wang, S., Han, P., Yan, K. "Electrode geometry optimization in wire-plate electrostatic precipitator and its impact on collection efficiency", Journal of Electrostatics, 80, pp. 76–84, 2016. https://doi.org/10.1016/j.elstat.2016.02.001

[26] Badran, M., Mansour, A. M. "Evaluating Performance Indices of Electrostatic Precipitators", Energies, 15(18), 6647, 2022. https://doi.org/10.3390/en15186647